

1 Article

## 2 Potential of Wind Energy Development for Water 3 Abstraction Systems in developing country context: 4 A case of Teso Sub-region of Uganda

5

6 Kasozi James Tondo<sup>1</sup>, Nicholas Kiggundu<sup>2,\*</sup>, Joshua Wanyama<sup>2</sup> and Noble Banadda<sup>2</sup>

7 <sup>1</sup> Department of Agriculture Infrastructure, Mechanization and Water for Production, Ministry of  
8 Agriculture Animal Industry and Fisheries, P.O Box 102, Entebbe, Uganda 1; jimkasoz@yahoo.com

9 <sup>2</sup> Department of Agricultural and Biosystems Engineering, Makerere University, P.O Box 7062, Kampala  
10 Uganda 2; [kiggundu@caes.mak.ac.ug](mailto:kiggundu@caes.mak.ac.ug), [wanyama2002@caes.mak.ac.ug](mailto:wanyama2002@caes.mak.ac.ug), [banadda@caes.mak.ac.ug](mailto:banadda@caes.mak.ac.ug)

11

12 \* Correspondence: [kiggundu@caes.mak.ac.ug](mailto:kiggundu@caes.mak.ac.ug); Tel.: +256-772-443-552

13

14 **Abstract:** Wind energy powered pumps could be an alternative to conventional fuel powered  
15 pumps for water abstraction because they rely on a free energy and they are environmentally  
16 friendly. The objective of this study was to assess the potential of wind energy to operate water  
17 abstraction systems in Teso sub-region of Uganda for livestock watering Daily mean wind speeds  
18 recorded at a height of 10 m for a period of ten years (2005-2015) were collected from Amuria and  
19 Soroti Meteorological stations in the study area. Data were analyzed using Weibull distribution to  
20 evaluate the annual wind speed frequency distributions and consequently assess their potential for  
21 water abstraction. The results indicated that warmer months (January, February and March) have  
22 higher mean wind speeds than the cold months (August, September and October). High wind  
23 speeds in the dry seasons corresponded to the periods of high water demand. The highest shape  
24 parameter (k) of 3.07 was registered in 2009 and scale parameter (c) of 3.78 in 2012. The highest  
25 wind power density of 43 W/m<sup>2</sup> was obtained the year 2012 while the lowest wind power density  
26 of 15.47 W/m<sup>2</sup> was obtained for Soroti district in the year 2009. The maximum power extractable in  
27 Amuria in 2012 was 324 W/m<sup>2</sup> which is potentially enough for water abstraction. Maximum  
28 discharges of 1.86 m<sup>3</sup>/s and 1.52 m<sup>3</sup>/s were obtained for Amuria and Soroti districts respectively at  
29 mean wind speeds of 5 m/s. Therefore, Teso sub region winds have potential for water abstraction  
30 and Amuria district better sites for livestock watering using wind energy.

31 **Keywords:** Wind energy; Weibull distributions; Water abstraction; Water stress; Water pumping

32

### 33 1. Introduction

34 Energy is vital for sustaining life on earth and plays a crucial role in human and economic  
35 development. As such energy poverty is one the injustices that call for human endeavor to address.  
36 Conventional energy sources (fossil fuels) are limited in nature, costly and when used cause  
37 greenhouse gas emissions [1-3] Global warming due to greenhouse gases contributed by us use of  
38 fossil fuels [4], calls for new strategies to utilize available renewable energy sources and wind energy  
39 is more promising [5-7]. However, accurate wind resource assessment is essential in the choice of a  
40 profitable location for harnessing wind power [8].

41 Teso sub-region in Northeastern Uganda is part of the cattle corridor and experiences water  
42 stress [9-11] regardless of the fact Uganda is endowed with abundant water resources [12-14]. Water  
43 scarcity in this region is largely driven by frequent and prolonged droughts, increasing livestock and  
44 human population growth leading to increasing water demand [15]. As a result, there is widespread  
45 of livestock diseases, increased nomadism and also social political conflicts. Interventions by  
46 Government of Uganda have focused on utilization of water resources for productive use through  
47 increasing storage volumes for water and exploitation of groundwater. Abstraction of water has  
48 relied on use of motorized pumps used at valley tanks, abstraction by gravity (used on dams),  
49 electric pumps and cattle ramp abstraction system. However, the systems have not been sustainable  
50 due to high operation costs of the conventional motorized pumps and limited access and high cost of  
51 electricity [16]. Only approximately 18.2 % of the total population in Uganda has access to the  
52 national power grid [17].

53 Wind energy powered pumps could be an alternative to conventional fuel powered pumps for  
54 water abstraction because they rely on a free energy source and are green-technology with an  
55 operational carbon-footprint of zero and thus environmentally friendly. However, its potential for  
56 water abstraction has not been assessed. The absence of reliable and accurate Uganda Wind Atlas,  
57 calls for further studies on the assessment of wind energy in potential areas in Uganda. Therefore,  
58 the overarching objective of this study was to assess the potential of wind energy to operate water  
59 abstraction systems in Teso sub-region of Uganda for livestock watering.

## 60 2. Materials and Methods

### 61 2.1 Description of Study area

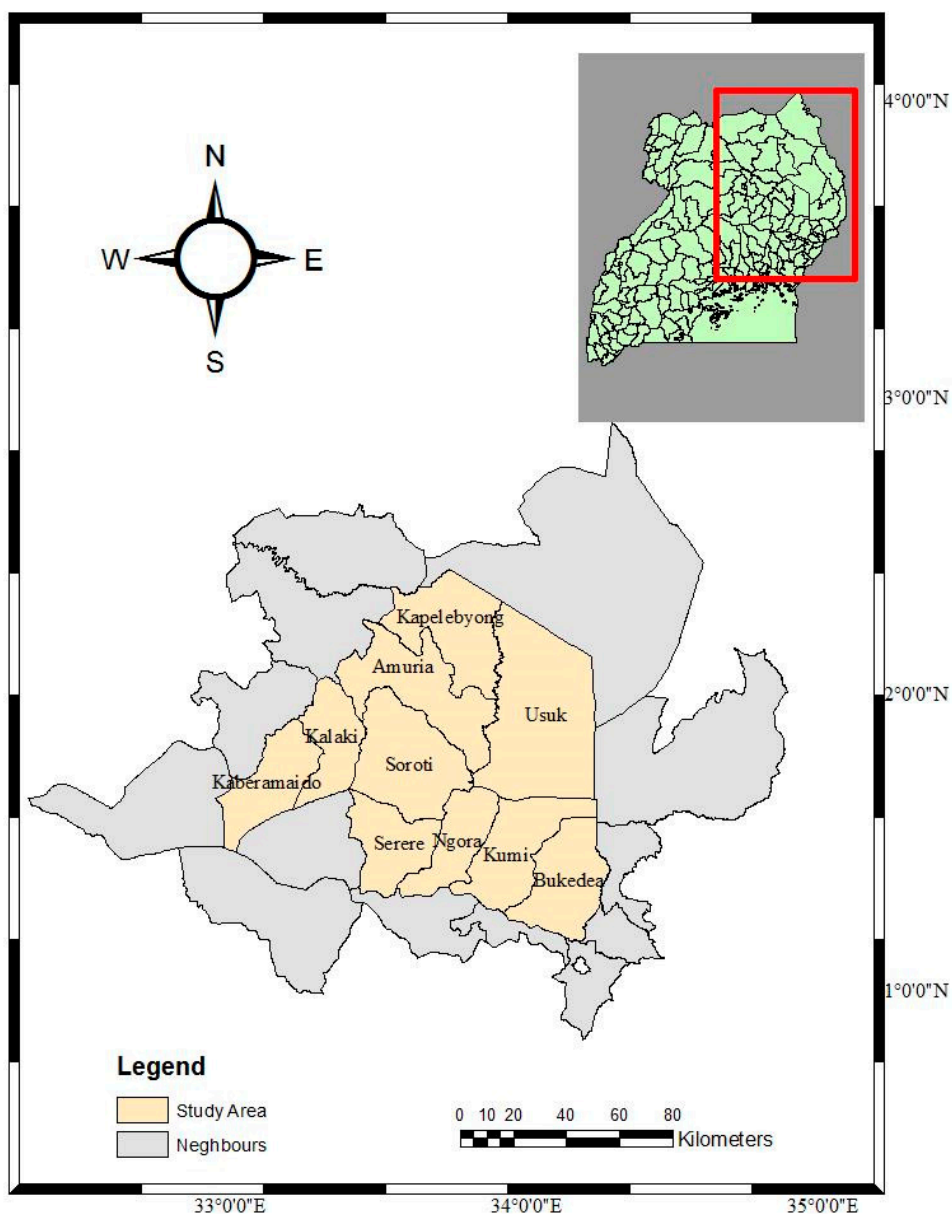
62 The study areas within Teso sub region were Amuria and Soroti districts as depicted in Figure  
63 1. Teso sub-region experiences a humid and hot climate, receiving bimodal rainfall with an annual  
64 average between 1,000 to 1,350 mm, much of which is received between March to May and  
65 Septembers to November. The main dry season begins in December and lasts till February. The  
66 climate of the sub-region is modified by the large swamp wetland area that surrounds it. Minimum  
67 and maximum temperatures are about 18°C and 31.3°C respectively. However, extremes usually  
68 occur in February, when the temperature can exceed 35°C. The vegetation is generally savannah.  
69 There are woodlands as well as forest plantations and reserves.

### 70 2.2 Data Analysis

71 According to the requirements for wind energy assessment, a representative year with  
72 maximum wind speed or peak is used to estimate the wind energy resource potential of a given  
73 study area [7].

#### 74 2.2.1 Weibull distribution function

75 The Weibull probability distribution function,  $f_w$  as shown in Equation 1 of different wind  
76 speeds of any region predicts the wind energy potential corresponding to different possible wind  
77 speeds in a certain period of time [18]. Weibull distribution is a two parameter function  
78 characterized by scale parameter  $c$  (m/s) and shape parameter  $k$  (dimensionless).  
79



80

81 **Figure 1.** A map showing the locations of the study areas in Teso sub region.

$$82 \quad f_w(v) = \left(\frac{k}{c}\right) \left(\frac{v}{c}\right)^{k-1} \exp\left[-\left(\frac{v}{c}\right)^k\right] \quad (1)$$

83 Where;  $k$  is the unit less shape parameter,  $c$  is the scale parameter in m/s and  $v$  is the Wind Speed84 The cumulative distribution function (Equation 2) is used to predict time at which a installed  
85 turbine actively functions in a given area [19]

$$86 \quad F_w(v) = 1 - \exp\left[-\left(\frac{v}{c}\right)^k\right] \quad (2)$$

87 Weibull parameters (Scale factor  $k$  and shape factor  $c$ ) for wind data analysis can be obtained  
88 using the Empirical method as given in the Equations 3 and 4 respectively.

$$89 \quad k = \left( \frac{\sigma}{\bar{v}} \right)^{-1.09} \quad (3)$$

$$90 \quad c = \frac{\bar{v}}{\Gamma\left(1 + \frac{1}{k}\right)} \quad (4)$$

91 Where  $\bar{v}$  is the mean wind speed and  $\sigma$  the variance of the known wind speed calculated using  
92 Equations 5 and 6 respectively and  $\Gamma$  is the gamma function and using the Stirling approximation the  
93  $\bar{v}$ gamma function of ( $x$ ) can be given as in Equation 7[19].

$$94 \quad \bar{v} = \frac{1}{n} \left[ \sum_{i=1}^n v_i \right] \quad (5)$$

$$95 \quad \sigma = \left[ \frac{1}{n-1} \sum_{i=1}^n \left( v_i - \bar{v} \right)^2 \right]^{\frac{1}{2}} \quad (6)$$

$$96 \quad \Gamma(x) = \int_0^{\infty} e^{-u} u^{x-1} du \quad (7)$$

### 97 2.2.2 Most probable wind speed

98 This refers to the most frequent wind speed for a given wind probability distribution Equation 8  
99 [19].

$$100 \quad V_{mp} = c \left( 1 - \frac{1}{k} \right)^{\frac{1}{k}} \quad (\text{m/s}) \quad (8)$$

### 101 2.2.3 Maximum energy carrying by the wind speed

102 The wind speed carrying maximum wind energy was calculated using Equation 9 [19].

$$103 \quad V_{\text{max}.E} = c \left( 1 + \frac{2}{k} \right)^{\frac{1}{k}} \quad (\text{m/s}) \quad (9)$$

### 104 2.2.4 Wind power density and Actual Power

105 Wind power density was determined to find a comparative measure of capacity of wind  
106 resource for the 2 districts (Amuria and Soroti). The power density was calculated using Equation 10  
107 [20, 21].

108 
$$P_m = \frac{1}{2} \rho c^3 \Gamma\left(\frac{k+3}{k}\right) \quad (10)$$

109 Where;  $P_m$  is the wind power density ( $W/m^2$ ),  $\rho$  is the air density =  $1.225 \text{ kg/m}^3$ ,  $v$  is wind velocity  
 110 (m/s),  $c$  is Weibull scale Parameter,  $k$  is Weibull shape parameter and  $\Gamma(x)$  is the gamma function of  
 111 (x).

112 The actual power was estimated using Equation 11 [22].

113 
$$Power = \frac{1}{2} \rho A V^3 \quad (11)$$

114 And taking swept area,  $A = 1 \text{ m}^2$

### 115 2.2.5 Wind energy density

116 Wind energy density was computed using Equation 12 which was derived from Equation 11 by  
 117 adding the desired time  $T$  as in accordance to Islam [19]. Equation 12 was very useful when  
 118 calculating the wind energy for any specific period when the achieved wind speed frequency  
 119 distributions were different.

120 
$$\frac{E}{A} = \frac{1}{2} \rho c^3 \Gamma\left(\frac{k+3}{k}\right) T \quad (12)$$

### 121 2.2.6 Weibull Wind Power Density

122 The wind power density was assessed using Weibull probability density function (pdf) given  
 123 by the expression in Equation 13 which have also been applied in similar studies [20, 21].

124 
$$P_w = \frac{1}{2} \rho c^3 \Gamma\left(1 + \frac{3}{k}\right) \quad (13)$$

125 Where:  $P_w$  is the Wind power Density,  $v$  is wind velocity (m/s),  $c$  is Weibull scale Parameter,  $k$  is  
 126 Weibull shape parameter,  $\Gamma(x)$  is the gamma function of (x).

### 127 2.2.7 Pump discharges with maximum mean wind speed and Power requirements

128 A year with maximum mean wind speed was used to calculate the power requirement of the  
 129 water abstraction system as well as coming up with the maximum pump discharges on a monthly  
 130 basis. The power requirement was computed using Equation 14 [22].

131 
$$P_u = 0.1 A_r (V_{mean})^3 \quad (14)$$

132 Where:  $P_u$  is the useful power delivered in pumping the water (W),  $A_r$  is the swept area of rotor ( $m^2$ )  
 133 and  $V_{mean}$  is the mean wind speed (m/s).

134 Since the commonly used systems for water abstraction in the Teso region is the piston pump  
 135 with a reciprocating motion, the instantaneous discharge  $Q_{vp}$  of the system at any velocity  $V$  can be  
 136 deduced as in Equation 15 [23].

$$137 \quad Q_{vp} = 2C_{pd}\eta(T,P)\frac{\rho_a\pi D_T^2}{\rho_w 4gH}V^3\left[1 - K_o\left(\frac{V_1}{V}\right)^2\right]K_o\left(\frac{V_1}{V}\right)^2 \quad (15)$$

138 Where:  $C_{pd}$  is the power coefficient of the rotor at the design point,  $\eta(T,P)$  is the combined  
 139 transmission and pump efficiency,  $K_o$  is a constant taking care of the starting behavior of the rotor  
 140 pump combination,  $\rho_a$  is the density of air (1.225 kg/m<sup>3</sup>),  $\rho_w$  is the density of water (1,000 kg/m<sup>3</sup>),  $H$   
 141 is the pressure head (approximately 5 m),  $V_1$  is the different mean wind speeds and  $V$  is the actual  
 142 mean wind speed of the study areas at reference height

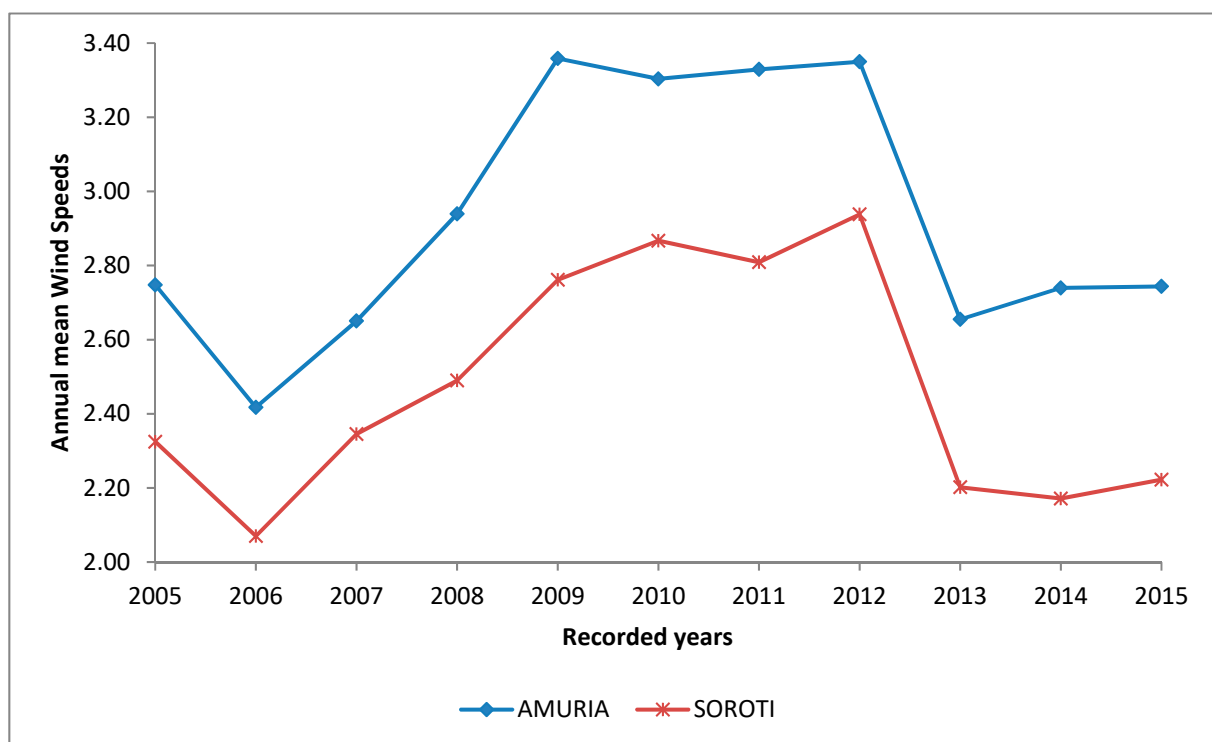
### 143 2.2.8 Wind energy potential for water abstraction

144 Microsoft excel software was used to evaluate the potential of the energy for water abstraction.  
 145 Minimum and maximum mean wind speeds for the study area were used as the input parameters to  
 146 compute the volumes of water that can be extracted and the correspond number of cattle watered.

## 147 3. Results

### 148 3.1 Mean wind speed

149 Figure 2 shows variations between the mean wind speeds (2005-2015) for the two study areas.  
 150 Overall, the mean wind speed for Amuria district was higher than that for Soroti district. The  
 151 highest mean speed in Amuria district was 3.35 m/s and lowest was 2.42 m/s in 2006. Soroti district  
 152 also registered high and low mean speeds in the same years as that of Amuria district. The lowest  
 153 wind speed was 2.07 m/s and highest was 2.94 m/s. There was a gradual decrease in wind speeds for  
 154 the two regions between 2005-2006 and then an exponential increase from year 2006 - 2012 where the  
 155 peak was obtained, after which it reduced in year 2013 and remained almost constant with small  
 156 variations between 2013 to 2015.



157

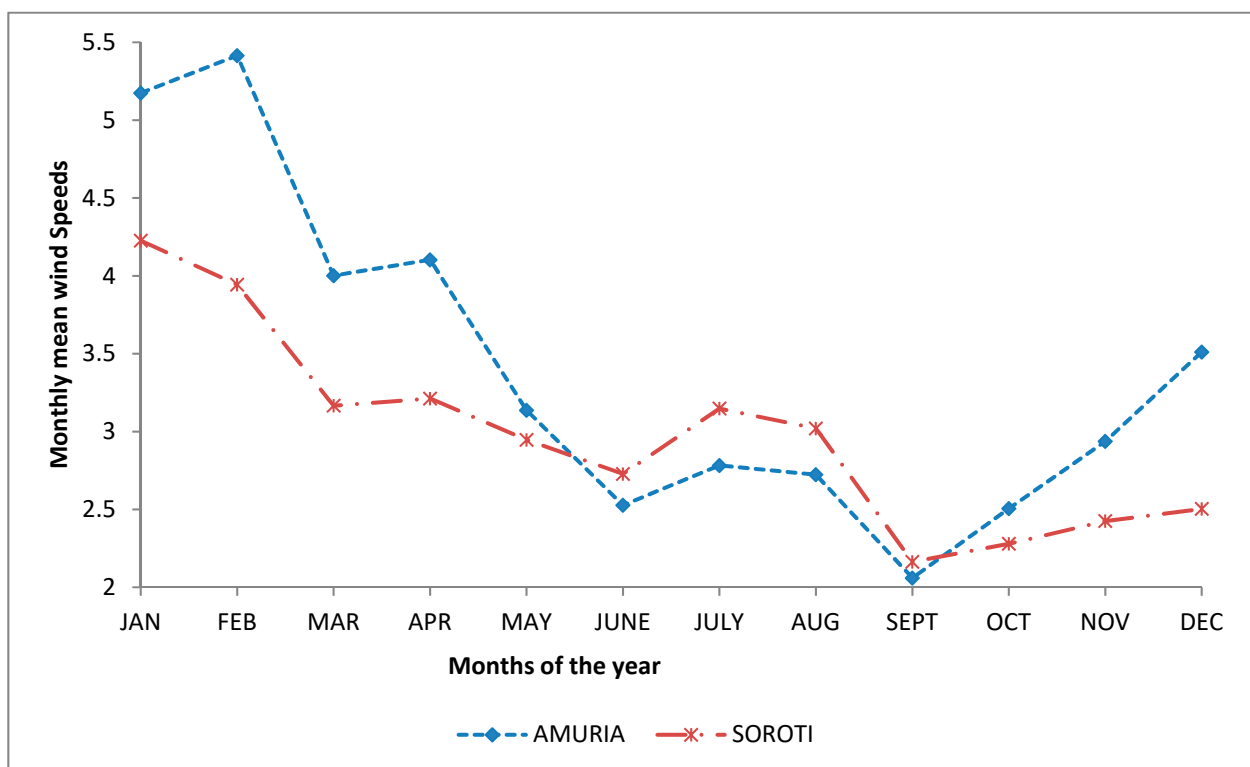
158

Figure 2. Annual wind Mean speeds for 10 year period

159 Figure 3 shows the monthly mean wind speed for the year 2012 because in all the study areas,  
 160 it's the year where the maximum wind speed or peak was achieved. For Amuria district, the highest  
 161 mean wind speed (5.41 m/s) was in February and the Lowest (2.06 m/s) in September. Soroti district  
 162 had the highest mean wind speed (4.23 m/s) in January and lowest (2.16 m/s) in September.

163 The mean wind speeds followed an exponential decreasing trend from January to June, then a  
 164 slight increase in June – August, then a decrease between August and September, thereafter a sharp  
 165 increase from September to December. The curves for the two study areas follow the same trend,  
 166 where wind speeds decreases from January to June and increases slightly from June to August then  
 167 reduces to September and increases again till December.

168 It is known that in the Teso region, dry months are January, February, June, July and December,  
 169 and in these months there is an increase in wind speeds at the onset of dry seasons (Figure 3) and  
 170 decrease in wind speed at the onset of cold seasons. The cold seasons in Teso region are March,  
 171 April, May, August, October and November.



172

173

Figure 3. Monthly wind speeds for 2012

### 174 3.2 Weibull Distribution

175 Table 1 shows the variations of the standard deviation, shape parameter (k), and scale  
 176 parameter (c) for four consecutive years (2009-2012) with the highest mean wind speeds for the  
 177 study areas.

178

179



180 **Table 1.** Annual mean wind speed, standard deviation, shape parameter (k), and scale parameter (c), Wind  
 181 power density (P<sub>m</sub>), Most Probable wind speed (V<sub>mp</sub>) and maximum energy carried by wind (V<sub>max.E</sub>)

Parameters	AMURIA					SOROTI				
	2009	2010	2011	2012	Average	2009	2010	2011	2012	Average
$\bar{v}$ (m/s)	3.36	3.30	3.33	3.35	3.34	2.76	2.87	2.81	2.94	2.85
$\sigma$ (m/s)	1.20	1.31	1.54	1.73	1.45	0.71	0.76	0.77	0.90	0.79
k	3.07	2.71	2.30	2.04	2.53	4.36	4.25	4.07	3.62	4.08
c (m/s)	3.76	3.71	3.76	3.78	3.75	3.03	3.15	3.10	3.26	3.14
P <sub>m</sub> (W/m <sup>2</sup> )	32.20	32.93	37.98	43.18	36.57	15.47	17.45	16.65	19.92	17.37
V <sub>mp</sub> (m/s)	0.83	0.86	0.92	0.94	0.89	0.54	0.57	0.57	0.65	0.58
V <sub>max.E</sub> (m/s)	2.02	2.38	3.05	3.68	2.78	1.01	1.09	1.13	1.40	1.16

182 *3.3 Monthly standard deviation, shape parameter (k), and scale parameter(c)*

183 The monthly standard deviation ranged from 1.20 to 1.73 m/s in Amuria district whereas Soroti  
 184 district had 0.71 to 0.90 m/s and one with the small difference in variation within standard deviation.

185 The range of variation of the shape parameters and scale parameters for Amuria is 2.04-3.07 and  
 186 3.71–3.78 m/s respectively and Soroti: 3.62–4.36 and 3.03–3.26 m/s respectively. The registered  
 187 highest shape parameter (k) was in 2009 and scale parameter (c) in 2012 for both Amuria and Soroti  
 188 districts.

189 *3.4 Wind power density, maximum energy carried by wind and most probable speed*

190 From Table 1, it was observed that the highest wind power density was 43.18 W/m<sup>2</sup> when the  
 191 two study areas were compared, and this density was obtained in Amuria district in year 2012. The  
 192 lowest wind density was 15.47 W/m<sup>2</sup> in Soroti district in 2009. The highest value of the wind speed  
 193 carrying maximum energy and most probable wind speed were 3.68 m/s and 0.94 m/s, and all  
 194 achieved in Amuria district in 2012.

195 At Amuria district in 2012, the maximum power extractable was equal to  $(0.598 \times 43.18 \text{ W/m}^2 \times$   
 196  $A)$  where A is the Swept area of the wind turbine. The used water abstraction wind powered  
 197 systems in Teso region have a swept radius of 2m, therefore area becomes,  $A = (\pi r^2) = (3.14 \times 2^2) =$   
 198  $12.56 \text{ m}^2$ . Finally the maximum power extractable at Amuria district if the peaks received are similar  
 199 with hose achieved in 2012 is 324.32 W.

200 *3.5 Weibull distribution and Cumulative distribution*

201 The Weibull parameters: scale parameter c (m/s) and shape parameter k (dimensionless) have  
 202 values computed on year basis (Table 1). For easy analysis, a year which registered peak mean wind  
 203 speed as well as highest scale parameter and shape parameter was selected and this was 2012. A plot  
 204 of probability distribution function,  $f_w(v)$  against wind speed was developed (Figure 3) with two  
 205 Study area – Amuria and Soroti districts found in Teso region.

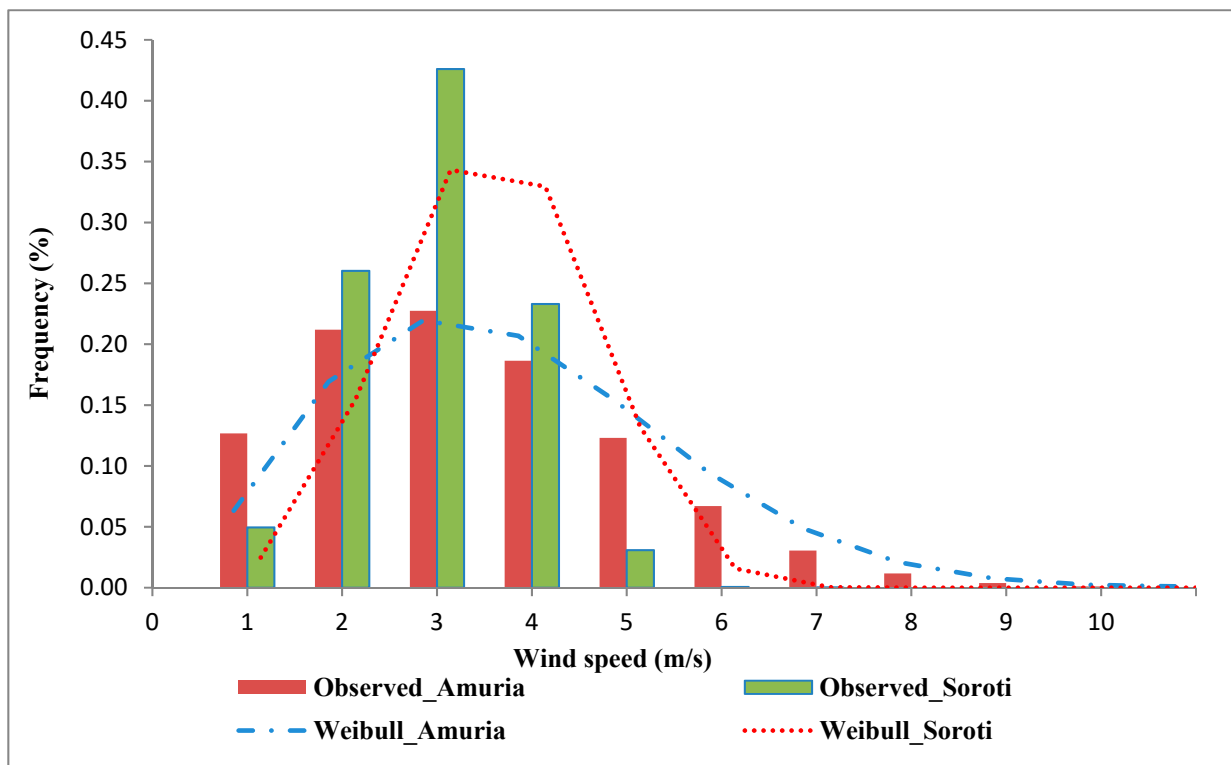
206

207

208



209



210

211 **Figure 4.** Weibull and Observed annual wind speed frequencies of Study areas in 2012

212 Figure 4 shows the annual variation of observed and Weibull wind speed frequencies for 2012  
 213 at Amuria and Soroti districts respectively. Maximum percentage error between Weibull and  
 214 observed frequencies occurs at less than 3 m/s wind speed at 23% for Amuria district and 43% for  
 215 Soroti district, and the maximum variation is 5% for all the study areas higher than 2 m/s.

216 *3.6 Maximum discharge of the pump with mean wind speeds*

217 Figure 5 indicates that maximum discharge is expected not beyond the mean wind speeds of 5  
 218 m/s, however according to the Weibull distribution the wind frequency is high at 3 m/s and therefore  
 219 the discharge can be 1.86 m<sup>3</sup>/hr and 1.52 m<sup>3</sup>/hr for Amuria and Soroti districts respectively. The  
 220 useful power delivered by the pump is 41.16 W for Amuria district and 25.57 W for Soroti district.  
 221 Therefore, more useful power delivered by the pump can happen when situated in Amuria district  
 222 because of the high mean wind speeds occurring in that region.

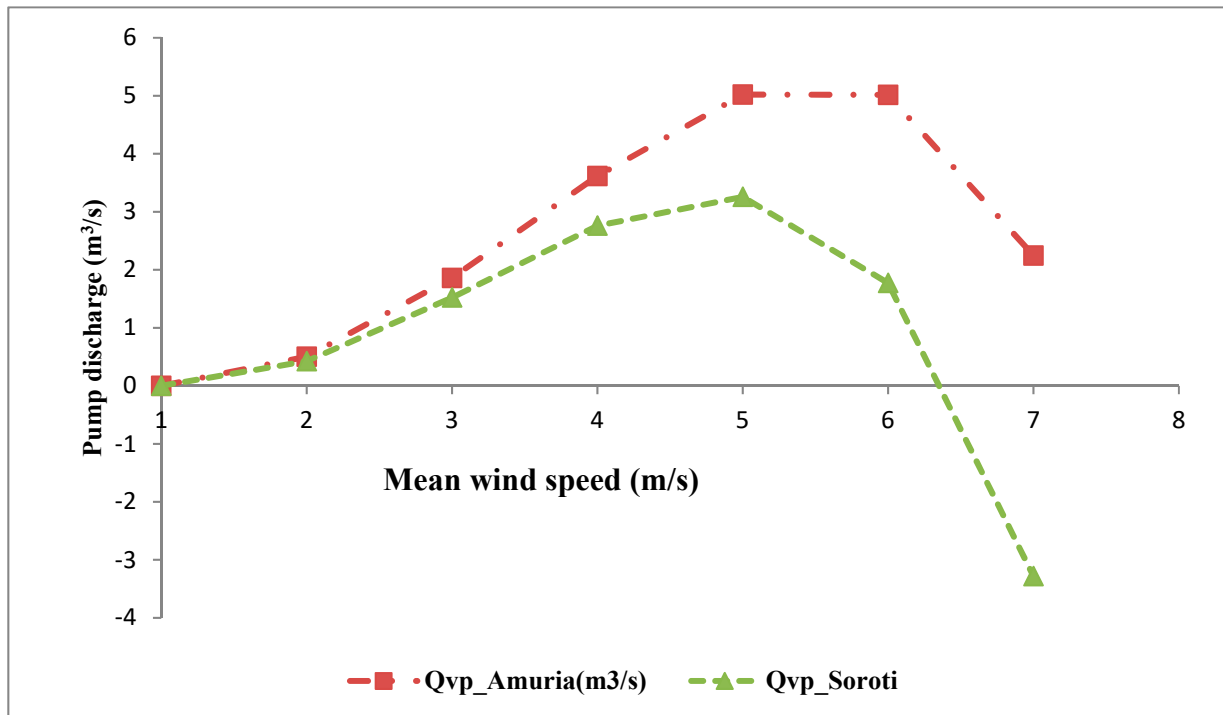


Figure 5. Maximum Pump discharge with different wind speeds

223

224

### 225 3.7 Wind energy potential for water abstraction

226 Results obtained from the computation of output power, discharge and the watered number of  
 227 cattle is shown in Table 2. It presents output power, discharge and the watered number of cattle for  
 228 the maximum and minimum speed among the series of 10 years data used for Amuria and Soroti  
 229 districts.

230 For Amuria, the discharge from the observed maximum and minimum mean wind speed was  
 231 2.79 m<sup>3</sup>/s and 2.01 m<sup>3</sup>/s respectively. The discharge as a result of maximum and minimum wind  
 232 speeds is able to water 1,743 and 1,255 heads of cattle respectively. For Soroti, the discharge from the  
 233 observed maximum and minimum mean wind speed was 2.79 m<sup>3</sup>/s and 2.01 m<sup>3</sup>/s respectively. The  
 234 discharge as a result of maximum and minimum wind speeds is able to water 1,743 and 1,255  
 235 number of cattle respectively considering a water demand of twenty (20) litres per day for local  
 236 cattle.

237 **Table 2.** Wind energy potential for water abstraction

Parameters	Amuria (m/s)		Soroti (m/s)	
	Maximum speed	Minimum Speed	Maximum speed	Minimum Speed
Output power (W)	23.23	8.68	15.57	5.43
Discharge (m <sup>3</sup> /s)	2.79	2.01	2.44	1.72
No of animals (Heads)	1743	1255	1525	1074

238

## 239 4. Discussion

240 There were observed differences in the wind speeds between the two study districts as seen in  
 241 Figure 2 and this could be attributed to a spatial climate variation [18]. Under a 'normal' climate

242 pattern for the study area, the lowest mean wind speeds should be expected in September (cold  
243 season) and the highest to be in months of January-February (hot season). Because inside a hot  
244 season, the air density is less than air density in the cold season, the observed wind speeds which  
245 depend on air density were as expected. The increase in wind speed during the dry seasons  
246 corresponds to the periods of high water demand in the study areas especially Amuria district at  
247 which high performance wind powered water abstraction systems is expected. According to  
248 Kaldellis [24], for most wind conditions,  $k$  always varies from 1.5 to 3, whereas  $c$  ranges from 3 to 8  
249 m/s. From Table 1, the average value of  $c$  is for the study areas (Amuria - 3.75 m/s; Soroti - 3.14 m/s)  
250 and the average value of  $k$  (Amuria – 2.53; Soroti – 4.08) were within the range observed by Kaldellis  
251 [24].

252 Since the shape parameter  $k$  determines the peak of the wind distribution, the analysis of this  
253 study shows that the wind distribution reaches the peak during dry periods of the year. Moreover,  
254 the ratio of  $k/c$  is a crucial factor in determining the peak frequency, and also predicting most  
255 probable speed with greater accuracy [18]. Authors Keyhani [2] suggested that the scale parameter  $c$   
256 indicates how windy a location is whereas the shape parameter  $k$  indicates how peaked the wind  
257 distribution is. Applying this argument to the analysis of this study points out that Amuria district is  
258 windier whereas Soroti district has the highest peaked wind distribution. Despite experiencing peak  
259 wind distribution required for maximum power output, Islam [19] found out that it is impossible for  
260 any device to convert all the output power to a usable form and so a Betz relation assigns a power  
261 coefficient of 0.593 for the maximum extractable power from an optimum wind energy conversion  
262 system.

263 According to Manwell [22], there is a range of power densities ( $P_m$ ) at which wind turbines can  
264 potentially function: If the  $P_m < 100$  W/m<sup>2</sup>, it is deemed a poor potential and if  $P_m \cong 400$  W/m<sup>2</sup>, it is  
265 deemed a good potential and for  $P_m > 700$  W/m<sup>2</sup>, it is great potential. For this study, the computed  
266 wind power potential tends to a good potential enough for water pumping.

267 In scenarios where there is observed zero or very low wind speed (less than 2 m/s) (Islam [19],  
268 the Weibull distribution is insufficient to represent probabilities. For this study, the observed  
269 distribution was reasonably well in the higher wind speed range (greater than 2 m/s) where  
270 maximum percentage error between frequencies is below 25%.

271 Using the cumulative distribution function which predicts the fraction of time a wind speed is  
272 below a particular speed and where a potentially installed wind powered abstraction system can be  
273 functional [7], the study established that for the wind turbine system to be functional at model mean  
274 wind speed of 3 m/s in the study area of Amuria district, it will be below this speed 46% of the time  
275 and in Soroti district, it will below the model speed 52% of the time. Using the peak mean wind  
276 speed received for each of the study areas: 3.35 m/s for Amuria district and 2.94 m/s for Soroti  
277 district all in the year 2012, the cumulative distribution of Amuria district would then be  
278 approximately 50% and for Soroti district 48%. Therefore from Table 2, Amuria district is endowed  
279 with more wind energy potential for abstracting water than Soroti district due to its higher pick  
280 mean winds.

## 281 5. Conclusions

282 The obtained results clearly show that warmer months have higher mean wind speeds than the  
283 cold months in all study areas. Therefore, the increase in wind speed in the dry seasons corresponds  
284 to the periods of high water demand in the study areas especially Amuria district at which high  
285 performance wind powered water abstraction systems is expected. The cold seasons in Teso region  
286 are March, April, May, August, October and November, and hot seasons in January, February,  
287 April, July and December.

288 The annual mean wind speeds for Amuria district were higher than that of Soroti district at 10  
289 m. The highest wind power density was 43.18 W/m<sup>2</sup> obtained in Amuria district in year 2012 and the  
290 lowest wind density was 15.47 W/m<sup>2</sup> in Soroti district in 2009. It is from the power density where  
291 maximum power extractable at Amuria district was achieved if wind speed peaks are received and  
292 occurred in 2012. The obtained power density was 324.32 W which is potentially enough to be used  
293 for pumping water.

294 The maximum discharge is expected not beyond the mean wind speeds of 5 m/s, however  
295 according to our Weibull distribution the wind frequency is high at 3 m/s and therefore the  
296 discharge can be 1.86 m<sup>3</sup>/s and 1.52 m<sup>3</sup>/s for Amuria and Soroti districts respectively. The useful  
297 power delivered by the pump is 41.16 W for Amuria district and 25.57 W for Soroti district.  
298 Therefore, more useful power delivered by the pump can happen when situated in Amuria district  
299 because of the high mean wind speeds occurring in that region.

300 Evaluation of the wind energy potential using the maximum and minimum mean wind speeds,  
301 results showed that discharges for both maximum and minimum speeds were high in Amuria than  
302 soroti. The discharge as a result of maximum and minimum wind speeds has the potential to water  
303 1743 and 1255 number of cattle respectively. The findings about the wind potential in water  
304 abstraction systems in Teso region, can be the future reference for engineers designing the wind  
305 pumps or those planning to set up pumps in Teso region.

306 **Author Contributions:** K.J.T. collected and analyzed the data, N.K. designed the research and wrote the paper,  
307 J.W analyzed part of the study and participated in the draft of the paper, N.B edited the paper.

308 **Funding:** This research received no external funding.

309 **Acknowledgments:** Weather Department of Soroti Flying School and Amuria Meteorological Center for  
310 availing weather.

311 **Conflicts of Interest:** The authors declare no conflict of interest.

## 312 References

- 313 1. Chauhan, D. Non-Conventional Energy Resources. **2006**, New Delhi: New Age International (P) Ltd.
- 314 2. Keyhani, A.; Ghasemi-Varnamkhashti, M.; Khanali, M. Abbaszadeh, R. An assessment of wind energy  
315 potential as a power generation source in the capital of Iran, Tehran. *Energy* **2010**. 35(1): 188-201.
- 316 3. Ohunakin, O.S. Akinnawonu, O.O. Assessment of wind energy potential and the economics of wind  
317 power generation in Jos, Plateau State, Nigeria. *Energy. Sust. Dev.* **2012**. 16(1): 78-83.
- 318 4. Sparks, D.; Madhlopa, A.; Keen, S.; Moorlach, M.; Dane, A.; Krog, P. Dlamini, T. Renewable energy  
319 choices and their water requirements in South Africa. *J. Energy South. Afr.* **2014**. 25(4): 80-92.
- 320 5. Khan, I.; Chowdhury, H.; Rasjedin, R.; Alam, F.; Islam, T. Islam, S. Review of wind energy utilization in  
321 South Asia. *Procedia Eng.* **2012**. 49: 213-220.

- 322 6. Shawon, M.; El Chaar, L.; Lamont, L. Assessments. Overview of wind energy and its cost in the Middle  
323 East. *Sust. Energy. Tech.* **2013**. 2: 1-11.
- 324 7. Al-Nhoud, O. Al-Smairan, M. Assessment of Wind Energy Potential as a Power Generation Source in  
325 the Azraq South, Northeast Badia, Jordan. *Mod. Mech. Eng.* **2015**. 5(03): 87.
- 326 8. Ouammi, A.; Sacile, R. Mimet, A. Wind energy potential in Liguria region. *Renew. Sust. Energ. Rev.*  
327 **2010**. 14(1): 289-300.
- 328 9. Mugerwa, S.; Stephen, K. Anthony, E. Status of livestock water sources in Karamoja sub-region,  
329 Uganda. *Resour. Environ.* **2014**. 4(1): 58-66.
- 330 10. Egeru, A.; Wasonga, O.; Kyagulanyi, J.; Majaliwa, G.M.; MacOpiyo, L. Mburu, J. Spatio-temporal  
331 dynamics of forage and land cover changes in Karamoja sub-region, Uganda. *Pastoralism* **2014**. 4(1): 6.
- 332 11. Mayega, R.W.; Tumuhamy, N.; Atuyambe, L.; Okello, D.; Bua, G.; Ssentongo, J. Bazeyo, W.  
333 Qualitative Assessment of Resilience to the Effects of Climate Variability in the Three Communities in  
334 Uganda. 2015 Available online:  
335 [http://www.ranlab.org/wp-content/uploads/2013/11/RAN\\_EA-RILab-Uganda-Community-Consultati](http://www.ranlab.org/wp-content/uploads/2013/11/RAN_EA-RILab-Uganda-Community-Consultations-Report-Climate.pdf)  
336 [ons-Report-Climate.pdf](http://www.ranlab.org/wp-content/uploads/2013/11/RAN_EA-RILab-Uganda-Community-Consultations-Report-Climate.pdf) [accessed 11 May 2017];
- 337 12. Water and Environment Sector and Performance Report. Available online:  
338 [library.health.go.ug/download/file/fid/1329](http://library.health.go.ug/download/file/fid/1329) [accessed 12 February 2016];
- 339 13. Nyenje, P.M. Batelaan, O. Estimating the effects of climate change on groundwater recharge and  
340 baseflow in the upper Ssezibwa catchment, Uganda. *Hydrolog. Sci. J.* **2009**. 54(4): 713-726.
- 341 14. Turton, A.R. Warner, J.F. Exploring the population/water resources nexus in the developing world. .  
342 **2002**, Washington, DC: The Woodrow Wilson Institute. pp. 52-81.
- 343 15. National Water Resources Assessment : report 2013. Available online:  
344 <https://searchworks.stanford.edu/view/11481686> [accessed 20 August 2017];
- 345 16. Kariuki, M. Schwartz, J. Small-scale private service providers of water supply and electricity: A review  
346 of incidence, structure, pricing, and operating characteristics. **2005**, Washington, DC: The World Bank.
- 347 17. Onyeji, I.; Bazilian, M. Nussbaumer, P. Contextualizing electricity access in sub-Saharan Africa.  
348 *Energy. Sust. Dev.* **2012**. 16(4): 520-527.
- 349 18. Parajuli, A. A statistical analysis of wind speed and power density based on Weibull and Rayleigh  
350 models of Jumla, Nepal. *Energy. Power. Eng.* **2016**. 8(07): 271.
- 351 19. Islam, M.; Saidur, R. Rahim, N. Assessment of wind energy potentiality at Kudat and Labuan,  
352 Malaysia using Weibull distribution function. *Energy* **2011**. 36(2): 985-992.
- 353 20. Ajayi, O.O.; Fagbenle, R.O.; Katende, J.; Ndambuki, J.M.; Omole, D.O. Badejo, A.A. Wind energy study  
354 and energy cost of wind electricity generation in nigeria: Past and recent results and a case study for  
355 south west nigeria. *Energies* **2014**. 7(12): 8508-8534.
- 356 21. Sharifi, F. Hashemi, N.N. An Analysis of Current and Future Wind Energy Gain Potential for Central  
357 Iowa. *J. Therm. Eng.* **2015**. 1(1): 245.
- 358 22. Manwell, J.F.; McGowan, J.G. Rogers, A.L. Wind energy explained: theory, design and application. 2  
359 ed. **2010**, Chichester, : John Wiley & Sons.
- 360 23. Mathew, S. Wind energy: fundamentals, resource analysis and economics. Vol. 1. **2006**, Berlin:  
361 Springer.
- 362 24. Kaldellis, J. The wind potential impact on the maximum wind energy penetration in autonomous  
363 electrical grids. *Renew. Energy* **2008**. 33(7): 1665-1677.